International Research Journal of Engineering and Technology (IRJET) e-ISSN: 2395-0056
Volume: 11 Issue: 10 | Oct 2024 www.irjet.net p-ISSN: 2395-0072

Coherence-based numerical differential current relay for synchronous generator stator windings protection

R. A. Mahmoud[1], E. S. Elwakil[2]

[1]Misr University for Science and Technology (MUST), College of Engineering Science & Technology, Department of Electrical Power and Machines Engineering (PME), 6th of October City-Giza-Egypt.
[2]Power Electronics and Energy Conversion Department, Electronics Research Institute, Cairo -Egypt.

Abstract:

A novel protective scheme for stator windings of synchronous generators is presented. The proposed method utilizes coherence coefficients for currents at both stator winding terminals to detect the fault condition in the AC power system, to determine which phase is faulty and to specify whether the fault is internal or external. The suggested scheme has developed closed-tripping characteristics to identify the relay tripping and blocking zones. Extensive fault situations are simulated using ATP software; then the protective scheme is verified using MATLAB package. In this method, the fault detection and classification are not affected by the fault types, fault locations, fault resistances, fault time span, fault inception times, and initial operating conditions. Moreover, it is smart and reliable; it can be practically implemented and gives fast time response (about half a cycle). In addition, the settings of the coherence coefficients can be selected in a narrow boundary. Besides, the proposed scheme can detect the ground faults near the neutral terminal of SG windings with high grounding impedance.

Keywords: Synchronous generator; Fault detection; Fault classification; Internal fault; External fault; Coherence coefficient.

1. Introduction

Due to the fact that Synchronous Generator (SG) is the most critical equipment in power networks, fault detection and classification are essential to avoid outages and blackouts [1-2]. As a result, many protection methods were proposed to protect SGs against various types of faults. Several researches and applications were processed for SGs protection in the literature. Faults in the SG are commonly classified as internal and external faults. The common internal faults may be phase to phase and phase to ground faults in stator windings, whereas external faults are those which occur outside the generator's protection zone, which may be caused by short circuits, over loading or unbalanced loads [3]. The conventional protection schemes consist of differential and stator earth-fault relays; those are known to be slow in clearing the faults unless the fault develops and current reaches the operating value [4]. Faults near neutral point, cannot be detected by earth-fault relays, especially for SG with high impedance grounding neutral due to insufficient voltage to drive the fault current [4]. To overcome these limitations, several techniques were proposed as in [5-7]. The paper in [7] presented a protection technique for stator windings against earth faults using the third harmonic voltage at the neutral and the terminals of the SG. Fault detection and classification schemes using statistical approaches such as correlation and alienation techniques were presented in [8-10]. SG protection methods based on signal processing techniques such as wavelet transforms were developed in [11-12]. Recently, Artificial Neural Network (ANN) technique was proposed for fault detection in SG stator windings [13]. The ANN technique is provided for detecting various internal, external and ground faults, which are close to neutral point. Other algorithms using a fuzzy logic controlled neural network were introduced in [14-17]; the algorithms utilized the fault generated transients for internal and external faults discrimination. The ANN and fuzzy logic were used for turn-to-turn fault detection, fault type classification and fault location identification [18-19]. In [20], the authors presented support vector machine-based fault detection and classification for electrical AC machines using vibration waves. Fault detection in Synchronous Generators (SGs) based on independent component analysis and machine learning was introduced in [21].

This paper presents a novel protection scheme for SG stator windings based on coherence analysis. The coherence coefficients are estimated for current signals measured at both terminals of three phase stator windings, which can be used for fault detection, faulty phase(s) selection, and fault location discrimination with respect to the generator protection zone. The proposed algorithm presents new tripping characteristic curves, utilizing coherence coefficients, to identify the relay tripping and blocking regions.

2. Synchronous generator modeling

Modeling of internal faults in synchronous generator cannot be built directly in the ATP program. When dynamics of the machine is not required, sinusoidal

voltage source model Type-14 can be used [22-23]. Thus, the package model Type-14 is easier for modeling SG to analyze the internal faults located on stator windings. In fact, the voltage source (Type-14) can be used for internal fault simulation during only the sub-transient period. The fault time interval of 3 cycles is sufficient for evaluating the proposed protection scheme. This was verified via the extensive case studies of ATP simulation presented in [23]. It has been proved that the short-circuit current, the 3-ph voltages and currents generated from three sources of Type-14 are identical to those obtained from the source of Type-SM59 during only the sub-transient period [24].

3. Proposed protection algorithm

3.1 Coherence index computation

$$Ci(k) = \frac{|\sum_{n=0}^{N-1} X(k) \times Y^*(k)|^2}{\sum_{n=0}^{N-1}|X(k)|^2 \times \sum_{n=0}^{N-1}|X(k)|^2} \quad (1)$$

$$X(k) = \sum_{n=0}^{N-1}\left[x(n)\cos(\frac{2\pi kn}{N})\right] - j\sum_{n=0}^{N-1}\left[x(n)\sin(\frac{2\pi kn}{N})\right] \quad (2)$$

$$Y(k) = \sum_{n=0}^{N-1}\left[y(n)\cos(\frac{2\pi kn}{N})\right] - j\sum_{n=0}^{N-1}\left[y(n)\sin(\frac{2\pi kn}{N})\right] \quad (3)$$

$$X(k) = a(k) - j\,b(k) \quad (4)$$

$$Y(k) = u(k) - j\,v(k) \quad (5)$$

Where,

Ci (*k*): The coherence coefficient calculated between the two time-series signals (*x(n)* and *y(n))* at a given frequency (*k*); the formula yields real value,

n: The sample number, n= 0, 1,...(*N*-1),

X(k): The Discrete Fourier Transform (DFT) of time-series signal ' *x(n)*'; the formula yields one complex number *X(k)* for every *k*,

Y(k): The Discrete Fourier Transform (DFT) of time-series signal ' *y(n)*'; the formula yields one complex number *Y(k)*for every *k*,

$$Ci(k) = \frac{\left[(\sum_{n=0}^{N-1} a(k)\times u(k)+b(k)\times v(k))^2+(\sum_{n=0}^{N-1} a(k)\times v(k)-b(k)\times u(k))^2\right]}{\sum_{n=0}^{N-1}[(a(k))^2+(b(k))^2]\times\sum_{n=0}^{N-1}[(u(k))^2+(v(k))^2]} \quad (6)$$

Where,

T_c: The cycle time period, (T_c= 20 *mSec*),

A coherence is a measure of the degree of relationship, as a function of frequency, between two time-series signals/sets. The coherence, sometimes called Magnitude-Squared Coherence (MSC), between any two signals/sets is a real-valued function; its values lie between 0.0 and +1.0 [25-26]. The magnitude of coherence is +1.0 if the two signals correspond to each other perfectly at a given frequency, (i.e. perfect coherent signals), while, if they are totally unrelated, the magnitude of coherence will be 0.0 (i.e. incoherent signals). If the coherence coefficient is less than one, but greater than zero, it indicates noise/harmonic content in the measurements. This means that the function relating the two signals is not linear. The coherence function can be described using the following mathematical formula [27-28]:

k: The frequency component number; *k* = 0, 1,...(*N*-1),

N: number of samples involved in one window,

j: The imaginary unit,

*: Denotes complex conjugation.

a(k): Cosine coefficient of the DFT for signal *x(n),*
b(k): Sine coefficient of the DFT for signal *x(n),*
u(k): Cosine coefficient of the DFT for signal *y(n),* and
v(k): Sine coefficient of the DFT for signal *y(n).*
The following mathematical equation represents the final form, used in the proposed algorithm, for calculating the coherence coefficient (*Ci* (*k*)):

$$\omega = \frac{2\pi k}{N} \qquad (Rad/Sec)$$

$$\omega = \frac{2\pi}{N.T_s} \qquad (Rad/Sec)$$

$$f = \frac{k}{N} \qquad (Hz)$$

$$f = \frac{1}{N.T_s} \qquad (Hz)$$

F_c: The fundamental frequency of one periodic cycle, (F_c= 50 *Hz*),

T_s: The sampling time interval, (T_s= 0.2 *mSec*),

F_s: The sampling frequency, (F_s= 5 *kHz*).

N_c: The number of samples per cycle for each signal ($x(n)$ and $y(n)$), ($N_c = T_c / T_s$ and $N_c = F_s / F_c$= 100 Samples/cycle).

3.2 Phase angle estimation

The calculated phase angle (φ_{12}) is directly related to the magnitude of coherence. If the phase angle is random between two time-series signals, then coherence coefficient is equal zero. When coherence is computed with a reasonable number of degrees and approaches unity, then the phase angle between the two time-series signals becomes meaningful because the interval of phase is a function of the coherence value and the degree of freedom. The phase relation determines, for two time-series signals, one is lag or lead from each other.

To estimate the phase shift angle (φ_{12}) between the two signals ($x(n)$ and $y(n)$) for every frequency component (k), the following equation can be applied [29]:

$$\varphi_{12}(k) = tan^{-1}\left[\frac{\sum_{n=0}^{N-1}[a(k) \times v(k) - b(k) \times u(k)]}{\sum_{n=0}^{N-1}[a(k) \times u(k) + b(k) \times v(k)]}\right] \quad (7)$$

Table 1: Coherence coefficient limits of current signals for different fault types and the relay action.

Fault location (for SG stator windings)	**Coherence coefficients limits**		**Fault classification type**		**Relay action**
	preset value of coherence $Cx = 1 - \Delta = 0.9$				
1. Normal operation	$1 \geq Ci_{a12} \geq Cx$, $1 \geq Ci_{b12} \geq Cx$, $1 \geq Ci_{c12} \geq Cx$ and $\Delta I \leq 20\% I_n$		No Fault		Blocking
2. External fault	$1 \geq Ci_{a12} \geq Cx$, $1 \geq Ci_{b12} \geq Cx$, $1 \geq Ci_{c12} \geq C$ and $\Delta I > 20\% I_n$		3LG or SLG or DLG or DL External Fault		Blocking
3. Internal fault	$Ci_{a12} < Cx$, $Ci_{b12} < Cx$ or $Ci_{c12} < Cx$	$Ci_{a12} < Cx$, $Ci_{b12} < Cx$ and $Ci_{c12} < Cx$	Internal Fault *3LG (A-B-C-G)*		Tripping
		$Ci_{a12} < Cx$, $1 \geq Ci_{b12} \geq Cx$ and $1 \geq Ci_{c12} \geq Cx$	Internal Fault, *SLG* phase 'A'		
		$1 \geq Ci_{a12} \geq Cx$, $Ci_{b12} < Cx$ and $1 \geq Ci_{c12} \geq Cx$	Internal Fault, *SLG* phase 'B'		
		$1 \geq Ci_{a12} \geq Cx$, $1 \geq Ci_{b12} \geq Cx$ and $Ci_{c12} < Cx$	Internal Fault, *SLG* phase 'C'		
		$Ci_{a12} < Cx$, $Ci_{b12} < Cx$ and $1 \geq Ci_{c12} \geq Cx$	Internal Fault *DLG (A-B-G) or* Internal Fault *DL (A-B)*	$1 \geq Ci_{ab} \geq Cx$ Internal Fault *DL (A-B), Otherwise* Internal Fault *DLG (A-B-G)*	
		$1 \geq Ci_{a12} \geq Cx$, $Ci_{b12} < Cx$ and $Ci_{c12} < Cx$	Internal Fault *DLG (B-C-G) or* Internal Fault *DL (B-C)*	$1 \geq Ci_{bc} \geq Cx$ Internal Fault *DL (B-C), Otherwise* Internal Fault *DLG (B-C-G)*	
		$Ci_{a12} < Cx$, $1 \geq Ci_{b12} \geq Cx$ and $Ci_{c12} < Cx$	Internal Fault *DLG (A-C-G) or* Internal Fault *DL (A-C)*	$1 \geq Ci_{ca} \geq Cx$ Internal Fault *DL (A-C) Otherwise* Internal Fault *DLG (A-C-G)*	

3.3 Proposed algorithm procedure

Fig. 1 presents the flow chart of the new protection scheme based on coherence coefficients. The algorithm performs three simultaneous tasks: fault detection, classification and localization. The procedure of the proposed algorithm can be described in the following steps:

(1) Read the sampled 3-phase currents signals at both ends of SG stator windings required to be protected (six current signals sampled at 5 kHz).

(2) Calculate the coherence coefficient (Ci_{s12}) for the two current signals ($i_{s1}(n)$ and $i_{s2}(n)$) measured at both stator winding ends of phase *'S'*. Each coefficient is estimated between each two corresponding windows of the two currents (i_{s1} and i_{s2}) of phase *'S'*.

(3) The sudden changes in the three coherence coefficient values can be analyzed and used to detect the fault condition, to identify the faulty phase(s) and to select the fault location.

(4) To discriminate between the DLG and DL faults, another three coherence coefficients (Ci_{ab}, Ci_{bc}, and Ci_{ca}) are required; they are computed between the two currents of the faulty phases taken at neutral or load side of SG stator windings. The coefficients (Ci_{ab}, Ci_{bc}, and Ci_{ca}) are evaluated for the three pairs of current signals (i_{a1} *(n)* and i_{b1} *(n))*, (i_{b1} *(n)* and i_{c1} *(n))* and (i_{c1} *(n)* and i_{a1} *(n)*), respectively.

(5) Also, the coherence coefficients (Ci_{ab}, Ci_{bc}, and Ci_{ca}) can be used to discriminate between normal operation and the fault conditions. Ideally, the values of these coefficients are *0.25* at normal operation. Hence if their values are out of the margin $0.25 \pm \Delta$, then the system condition is faulty.

(6) The action of the protection algorithm follows the listed conditions in Table 1.

3.4 Proposed tripping-characteristics design

Figs. 2(a-c) present the characteristics of the proposed protective algorithm. Each characteristic is depicted for each pair of coherence coefficients for current signals. The characteristic has two zones: a blocking zone for normal operation or external fault condition and a tripping zone for internal fault condition. The processes of fault detection, faulty phase(s) identification and fault location discrimination (internal or external) start altogether in parallel with a maximum execution time of 10 mSec (i.e. half a cycle).

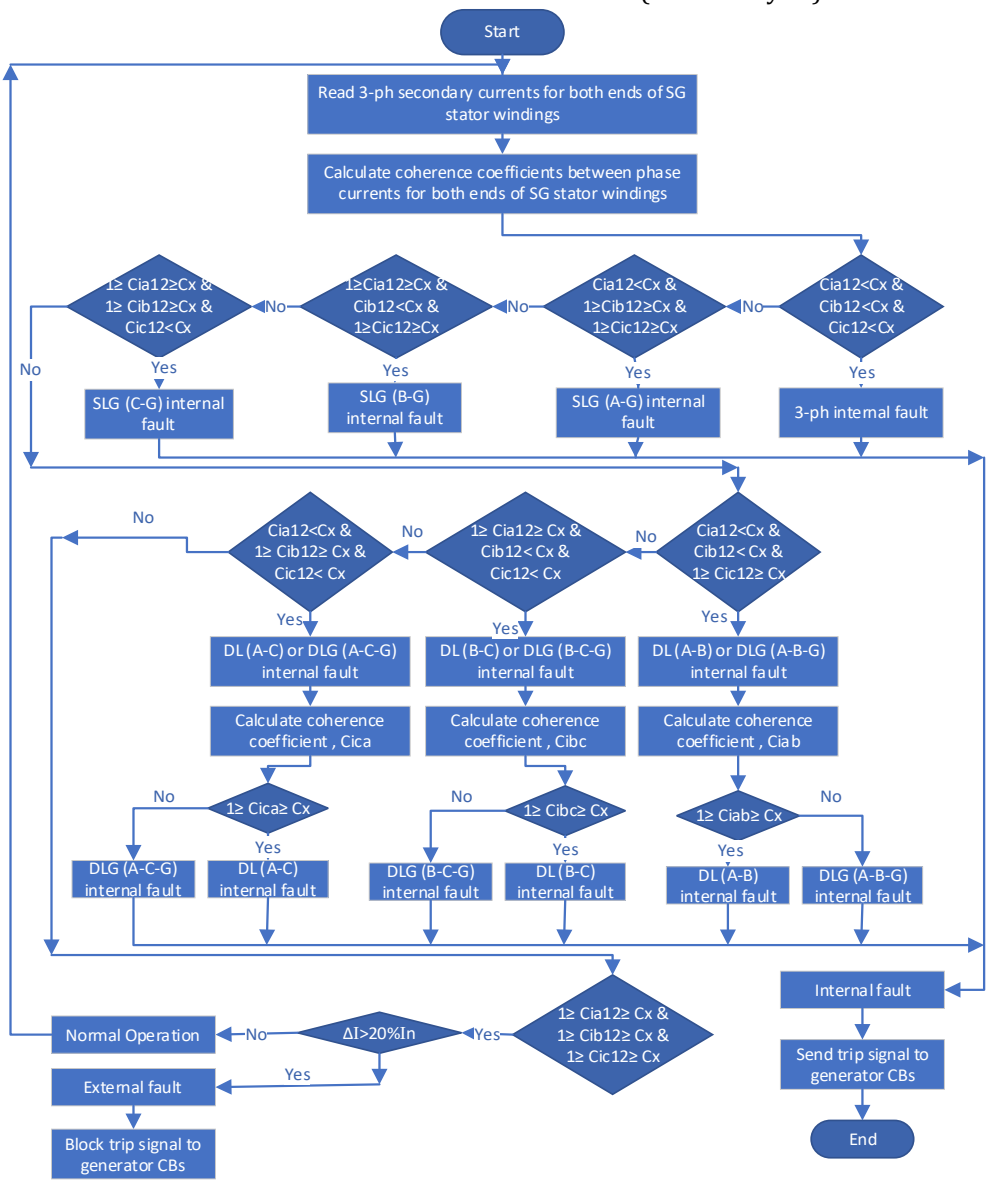

Fig. 1: Flow chart of the proposed algorithm.

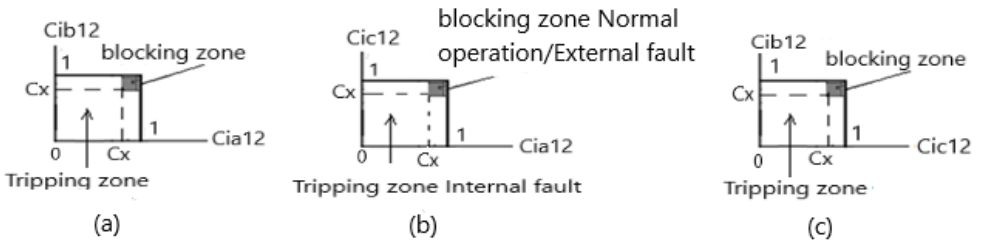

Figs. 2(a-c): Tripping characteristics.

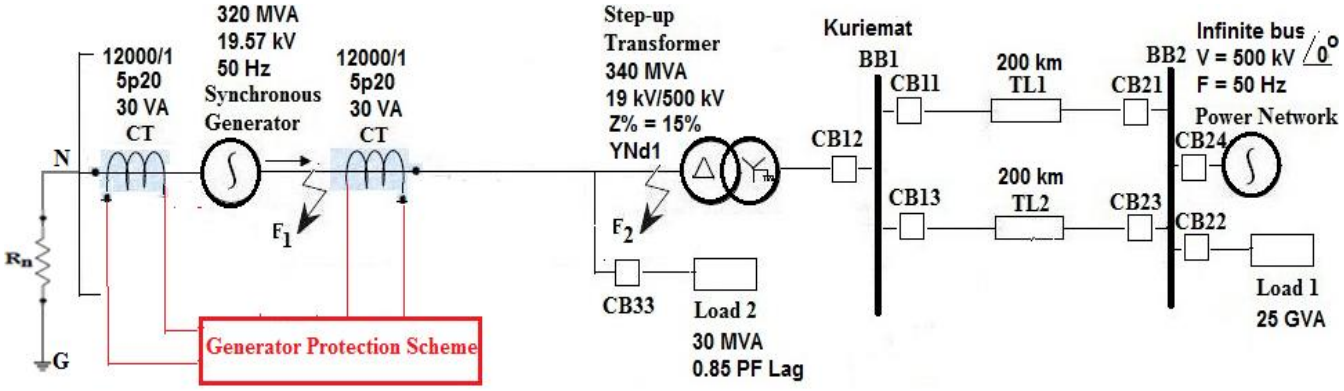

Fig. 3: Synchronous generator connected to a power system network.

4. Simulated power system

A power system model consisting of a synchronous generator, which feeds the loads through a step down transformer and double circuits of transmission lines, is considered for simulation. The model is shown in Fig. 3. The pre-fault operating conditions and parameters of the simulated power system are given in Appendix 1 and Appendix 2 [29].

5. Simulation findings and analysis

Different types of short circuits have been simulated and tested using ATP and MATLAB for the case studies of sections 5.1 to 5.4 considering different fault types, fault locations (0-100%) on stator windings, fault resistances (0-20 Ω), fault inception angles (0-90°) and fault zones (internal/external). The total simulation time is 0.2 Sec (i.e. N_{sim} = 1000 samples); and the fault inception time is set to t_f = 0.102 Sec (i.e. N_f = 510 samples). It is assumed that the SG is loaded before the fault inception. The sampling frequency is f_s = 5.0 kHz (i.e. h = 0.0002 Sec).

5.1 Case 1: SLG external fault

A single line-to-ground (*SLG*) fault is inserted at the location of point F_2 between the primary side of the step-up transformer and load 2. For this case, the fault resistance is 1 Ω, the grounding impedance of the generator neutral point is 1 Ω and the fault inception angle is 36°. Fig. 4(a-c) show the 3-phase secondary currents at both terminals of SG stator windings. The current magnitudes during fault are higher than the pre-fault current magnitudes for the two phases A' and 'B'; while the current magnitude of phase 'C' during fault is lower than the pre-fault current. This is due to the *SLG* external fault located on the phase 'A' and the delta connection of the primary windings of the transformer. The two current signals, at the ends of stator windings, are identical before and after the fault inception time. Fig. 4(d) shows the delay angles (Ti_{a12}, Ti_{b12} and Tic_{12}) evaluated between the three pairs of phase currents. It is observed that the three angle differences are zero degrees because the fault location is external. The 3-phase coherence coefficients (Ci_{a12}, Ci_{b12} and Ci_{c12}) are shown in Fig. 5(a) to be equal and close to one before and after the fault instant. The values of these coefficients confirm that the system condition is either external or normal operation. The calculated values of coherence coefficients (Ci_{ab}, Ci_{bc}, and Ci_{ca}) are balanced and close to 0.25 before the fault starting. While they are unbalanced during fault with values between 0 and 0.8, as shown in Fig. 5(b). Thus, these unbalanced values prove that the fault is external. The proposed technique prevents the tripping of generator CB(s) in the case of external fault condition. Fig. 5(c) shows the blocking flag, which is zero in this case. Fig. 5(d) shows the operating point on the characteristics due to the SLG external fault. It is noticed that the values of (Ci_{a12}, Ci_{b12} and Ci_{c12}) on the three characteristics are identical and located at the value of one.

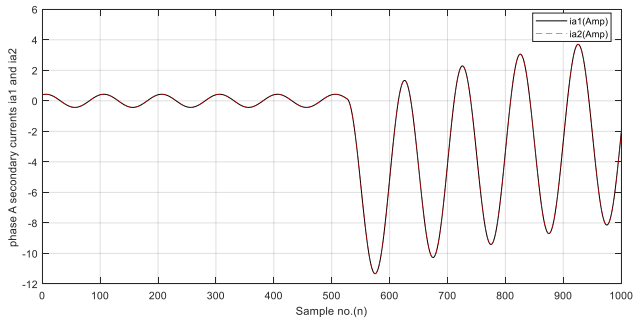

Fig. 4(a): Current signals i_{a1} and i_{a2}.

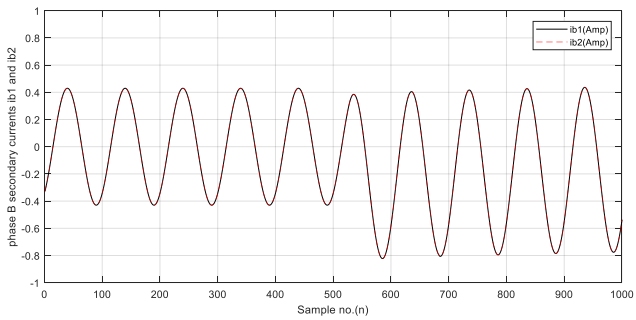

Fig. 4(b): Current signals i_{b1} and i_{b2}.

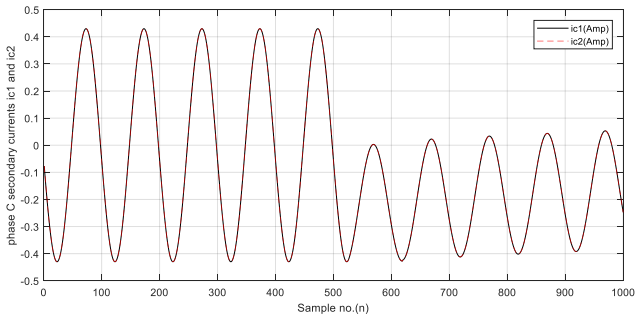

Fig. 4(c): Current signals i_{c1} and i_{c2}.

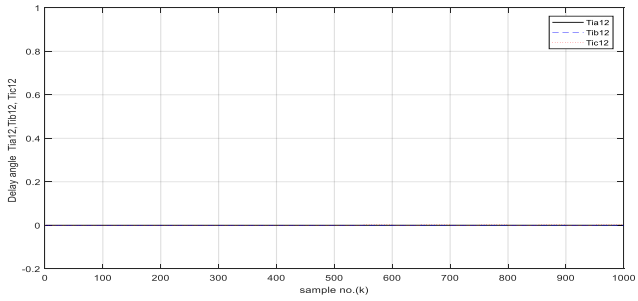

Fig. 4(d): Delay angles between the two current signals of each phase.

Fig. 4(a-d): Current signals taken at the terminals of SG stator windings and their delay angles for case 1.

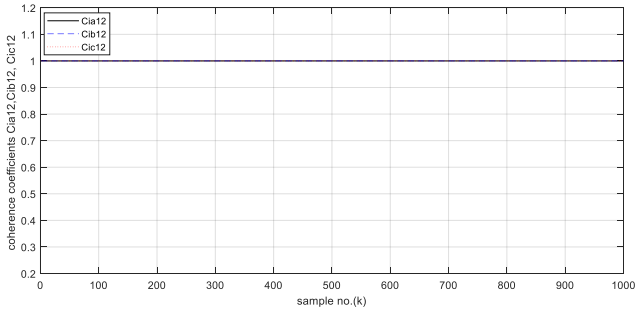

Fig. 5(a): Coefficients (Ci_{a12}, Ci_{b12} and Ci_{c12}).

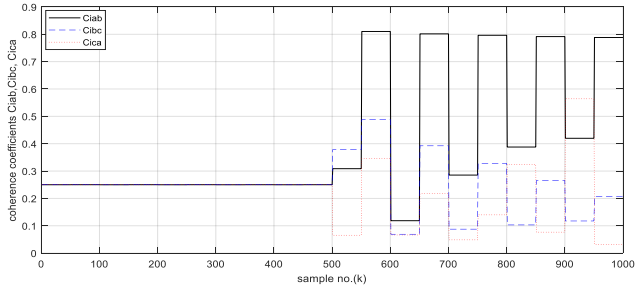

Fig. 5(b): Coefficients (Ci_{ab}, Ci_{bc} and Ci_{ca}).

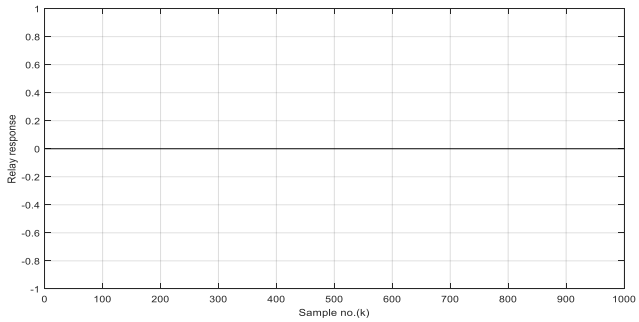

Fig. 5(c): Blocking flag in case 1.

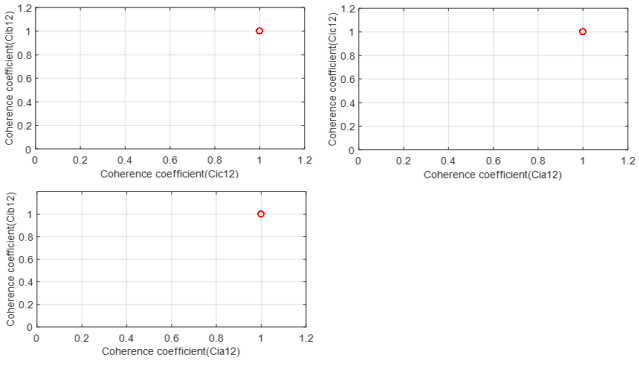

Fig. 5(d): Proposed scheme blocking on the tripping characteristics.

Fig. 5(a-d): Simulation results of case 1.

5.2 Case 2: SLG fault at 100% phase 'A' of stator winding

A SLG internal fault is simulated at 100% of stator windings away from the neutral point. In this case, the fault location is changed to SLG internal fault on phase 'A' through a fault resistance R_f = 1 Ω. Fig. 6(a-c) presents the curves of three-phase secondary currents at both stator windings terminals. The two phase-current's magnitudes of the healthy phases; '*B*' and '*C*', before and during the fault interval, are identical. The current magnitude of i_{a1}, for the faulty phase '*A*', during the fault period is higher than i_{a2} and the pre-fault current magnitudes. Fig. 6(d) shows the shift angle deviations (Ti_{a12}, Ti_{b12} and Tic_{12}) evaluated between the three pairs of the three phase currents, at both stator winding ends, respectively. The three angle differences are zero before the fault occurrence. During fault, Ti_{a12} is greater than 70°, while Ti_{b12} and Tic_{12} remain zero because the fault type is SLG internal fault for phase 'A'. The calculated six coherence coefficients (Ci_{a12}, Ci_{b12}, Ci_{c12}, Ci_{ab}, Ci_{bc}, and Ci_{ca}), the tripping signal, the proposed scheme operation on the tripping characteristics are shown in Fig. 7(a-d). The calculated values of the three coherence coefficients (Ci_{a12}, Ci_{b12} and Ci_{c12}) are fixed close to one before fault inception. During fault period, the values of coefficients (Ci_{b12} and Ci_{c12}) are still fixed; whereas the values of the coefficient (Ci_{a12}) lie between the values of 0 and 0.8, as shown in Fig. 7(a). The values of coherence coefficients (Ci_{a12}, Ci_{b12} and Ci_{c12}) prove that the system load is balanced before fault inception and the fault type is SLG internal fault on the phase 'A'. The estimated values of coherence coefficients (Ci_{ab}, Ci_{bc}, and Ci_{ca}) are fixed at 0.25 before the fault time, but they are unsymmetrical during fault, where their values range between 0 and 1.0, (see Fig. 7(b)). Thus, the six coherence coefficients confirm that the system status is internal fault. A tripping signal is sent for isolating the generator CB(s) as shown in Fig. 7(c). The operating points on the tripping characteristics in case of SLG internal fault are depicted in Fig. 7(d).

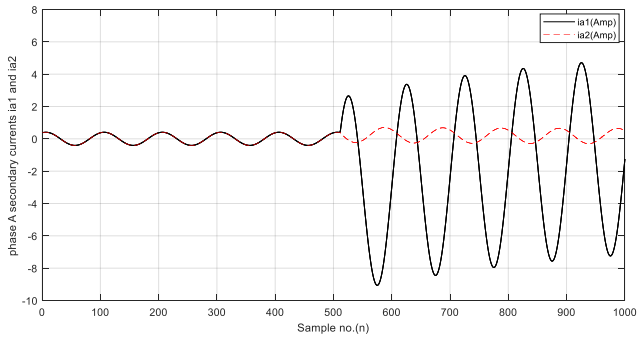

Fig. 6(a): Current signals i_{a1} and i_{a2}.

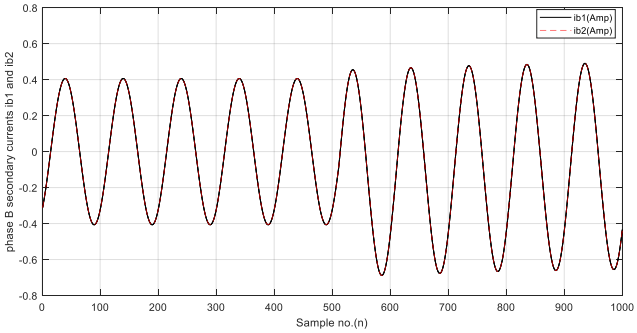

Fig. 6(b): Current signals i_{b1} and i_{b2}.

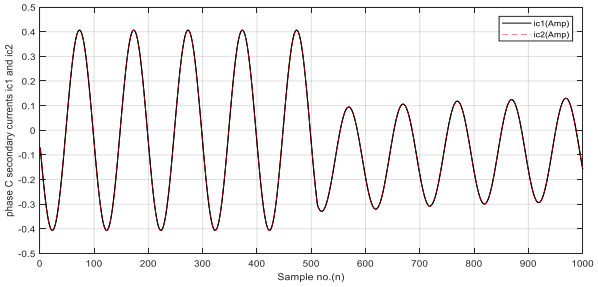

Fig. 6(c): Current signals i_{c1} and i_{c2}.

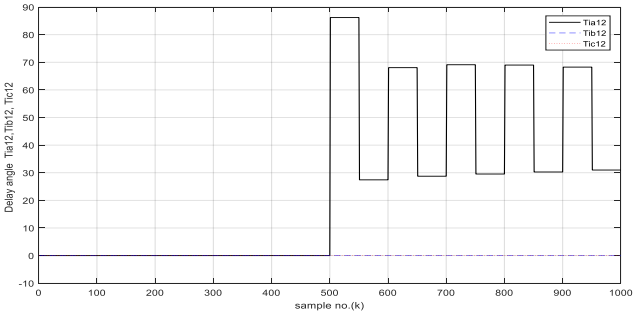

Fig. 6(d): Delay angles between the two current signals of each phase.

Fig. 6(a-d): Current signals taken at both terminals of SG stator windings and their delay angles for case 2.

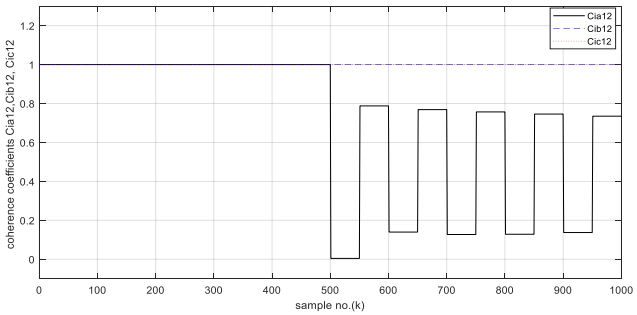

Fig. 7(a): Coefficients (Ci_{a12}, Ci_{b12} and Ci_{c12}).

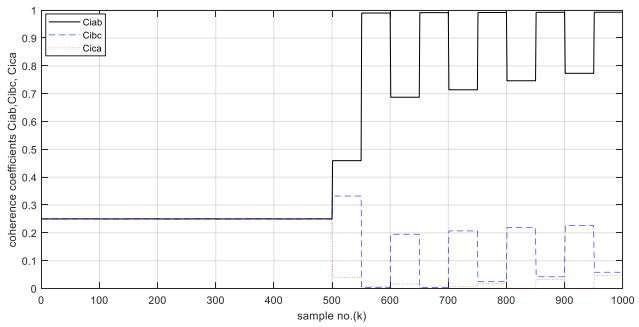

Fig. 7(b): Coefficients (Ci_{ab}, Ci_{bc} and Ci_{ca}).

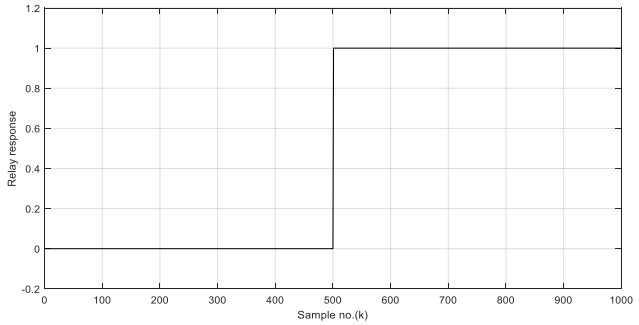

Fig. 7(c): Tripping flag in case 2.

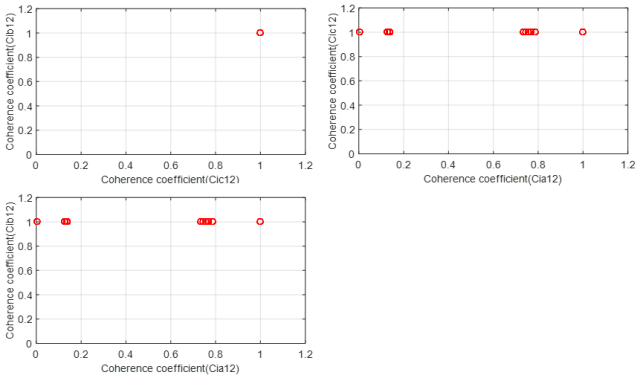

Fig. 7(d): Proposed scheme operating point on the tripping characteristics.

Fig. 7(a-d): Simulation results for case 2.

5.3 Case 3: SLG fault at 10% phase 'A' of stator winding

In this case, a SLG fault is placed 10% away from the neutral point of phase '*A*' winding with a fault resistance of 1 Ω. The algorithm has correctly classified the fault incident as an internal fault. This is proven in the simulation results explained in this case. Fig. 8(a-c) shows the three pairs of secondary currents at neutral and load sides for SG stator windings. The current signals of phases 'B' and 'C' obtained at stator winding ends are identical and their magnitudes during fault time are the same magnitude of the pre-fault current. It can be noticed that the current signals (i_{a1} and i_{a2}) of the faulty phase '*A*' at both ends of the stator winding are not similar. The current amplitude of i_{a2} are larger than the current amplitude of i_{a1} as shown in Fig. 8(a). The estimated coherence coefficients (Ci_{a12}, Ci_{b12}, Ci_{c12}, Ci_{ab}, Ci_{bc}, and Ci_{ca}), the tripping signal and the scheme operating point on the tripping characteristics are introduced in Fig. 9(a-d). The calculated values of coherence coefficients (Ci_{a12}, Ci_{b12} and Ci_{c12}) are fixed at one before fault inception. For the faulty phase 'A', Ci_{a12} is less than *0.1* during fault period. While the coherence coefficients of Ci_{b12} and Ci_{c12} remain at the value one during fault, as shown in Fig. 9(a). The calculated values of coherence coefficients (Ci_{ab}, Ci_{bc}, and Ci_{ca}) are balanced and close to 0.25 before fault, while they are unbalanced during fault (see Fig. 9(b)). The condition of the SLG fault at 10% of phase 'A' winding leads to a trip signal to be sent for isolating the generator CB(s) with the fault beginning, at the sample number of 510 as shown in Fig. 9(c). The operating points in this case are plotted on the tripping characteristics in Fig. 9(d).

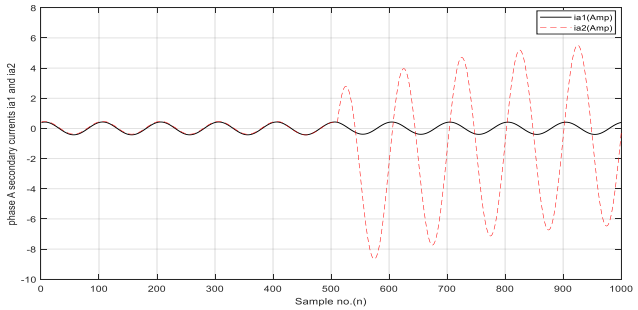

Fig. 8(a): Current signals i_{a1} and i_{a2}.

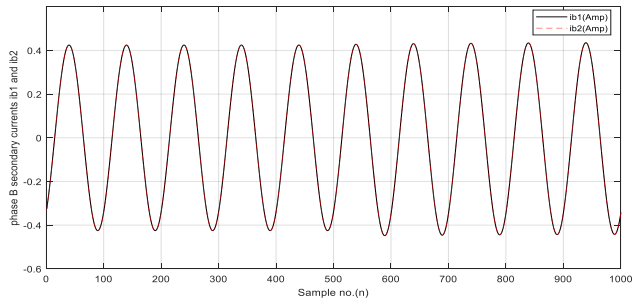

Fig. 8(b): Current signals i_{b1} and i_{b2}.

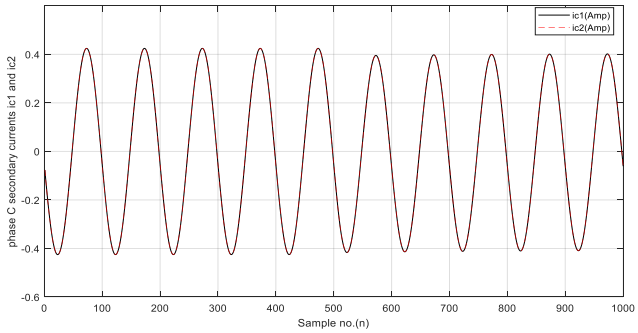

Fig. 8(c): Current signals i_{c1} and i_{c2}.

Fig. 8(a-c): Current signals taken at both terminals of SG stator windings for case 3.

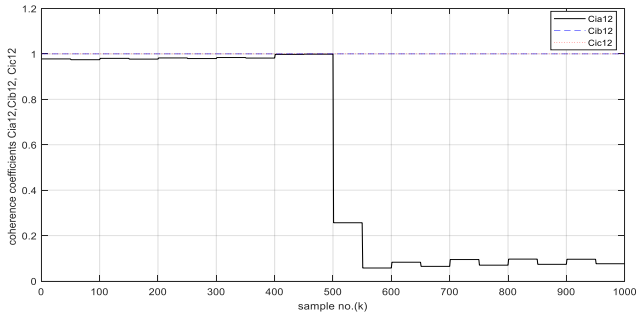

Fig. 9(a): Coefficients (Ci_{a12}, Ci_{b12} and Ci_{c12}).

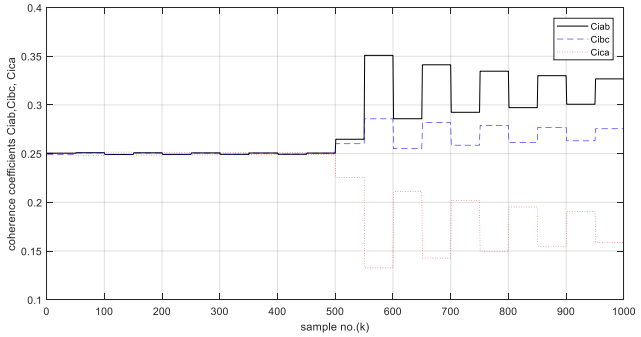

Fig. 9(b): Coefficients (Ci_{ab}, Ci_{bc} and Ci_{ca}).

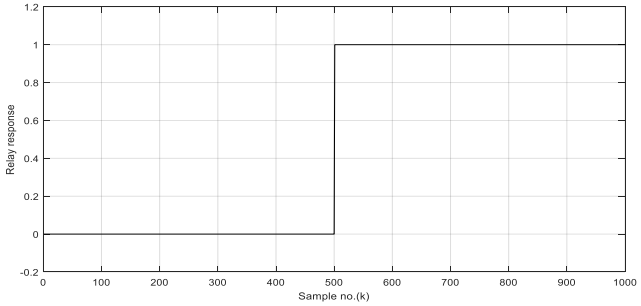

Fig. 9(c): Tripping flag in case 3.

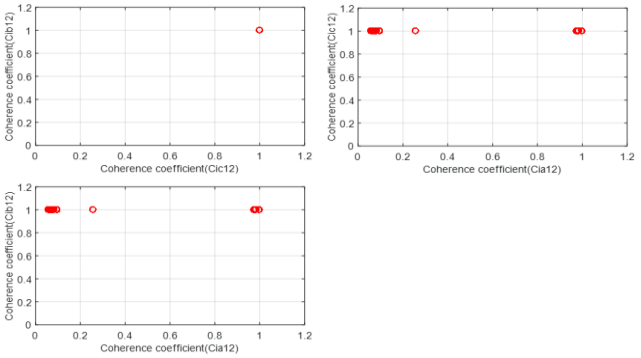

Fig. 9(d): Proposed scheme operating points on the tripping characteristics.

Fig. 9(a-d): Simulation results for case 3.

5.4 Case 4: SLG fault at 5% of phase 'A' stator winding

This is a case of an internal SLG fault occurred at 5% of phase '*A*' stator winding away from the neutral point and the fault resistance is 1 Ω. Fig. 10(a-c) presents the waveforms of the 3-phase secondary currents at neutral and load sides for SG stator windings. It can be observed that the current signals (i_{a1} and i_{a2}) of the faulty phase '*A*' at the ends of the stator windings are different. The current i_{a2} has a larger value due to the short circuit occurrence. Whereas the phase current magnitudes of the healthy phases '*B*' and '*C*' during fault are identical with approximately the same values as those of the pre-fault current. Fig. 11(a-d) shows the estimated six coherence coefficients (Ci_{a12}, Ci_{b12}, Ci_{c12}, Ci_{ab}, Ci_{bc}, and Ci_{ca}), the tripping signal, and the operating protection scheme on the tripping characteristics, respectively. The calculated values of the coherence coefficients (Ci_{a12}, Ci_{b12} and Ci_{c12}) are constant and close to one before the fault inception time. During the fault period, the values of Ci_{b12} and Ci_{c12} are fixed and close to one whereas Ci_{a12} values are less than *0.2*, as shown in Fig. 11(a). The values of the coherence coefficients (Ci_{ab}, Ci_{bc}, and Ci_{ca}) are equal and close to 0.25 before fault, while they are greater than *0.27*during fault, as shown in Fig. 11(b). The values of (Ci_{a12}, Ci_{b12} and Ci_{c12}) confirm that the fault type is SLG internal fault and the values of (Ci_{ab}, Ci_{bc}, and Ci_{ca}) indicate to existing unbalance condition for the three phase currents of the stator windings. Due to the internal fault event, a tripping signal is issued to isolate the protected generator. The scheme sets a trip signal for opening the generator CB(s), as shown in Fig. 11(c). Fig. 11(d) shows the scheme operation on the tripping characteristics in the case of SLG fault at 5% of phase 'A' stator winding. The response of the coherence function, in this case and in the previous cases, proved that the proposed technique is able to determine the healthy and faulty phases and discriminate between the internal and external faults.

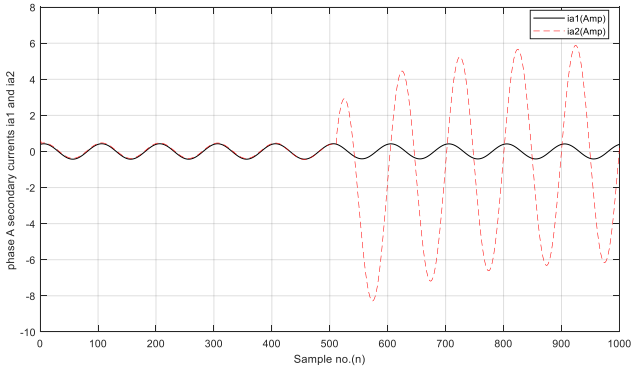

Fig. 10(a): Current signals i_{a1} and i_{a2}.

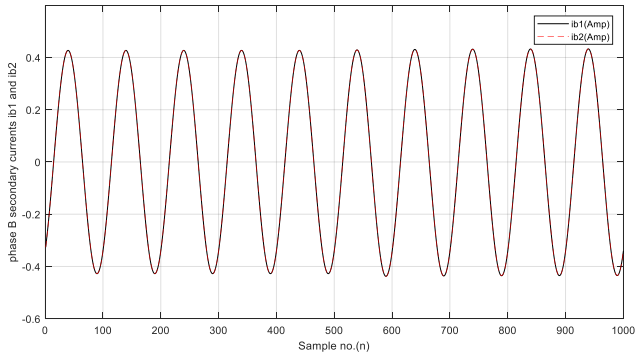

Fig. 10(b): Current signals i_{b1} and i_{b2}.

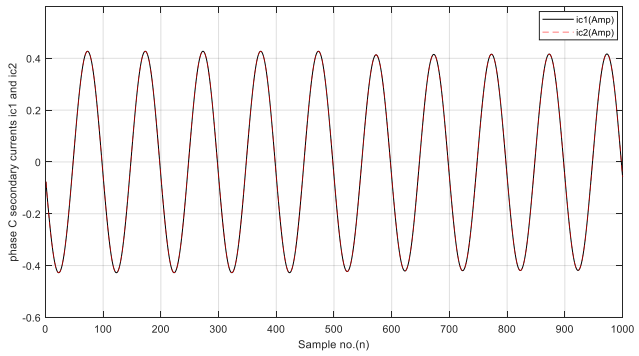

Fig. 10(c): Current signals i_{c1} and i_{c2}.

Fig. 10(a-c): Current signals taken at both terminals of SG stator windings for case 4.

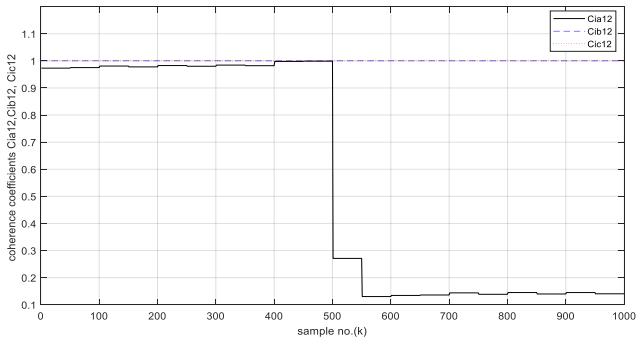

Fig. 11(a): Coefficients (Ci_{a12}, Ci_{b12} and Ci_{c12}).

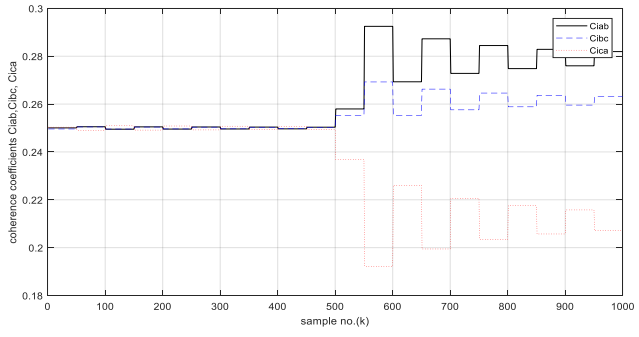

Fig. 11(b): Coefficients (Ci_{ab}, Ci_{bc} and Ci_{ca}).

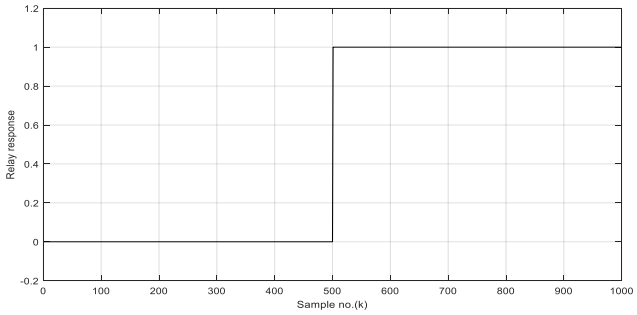

Fig. 11(c): Tripping flag in case 4.

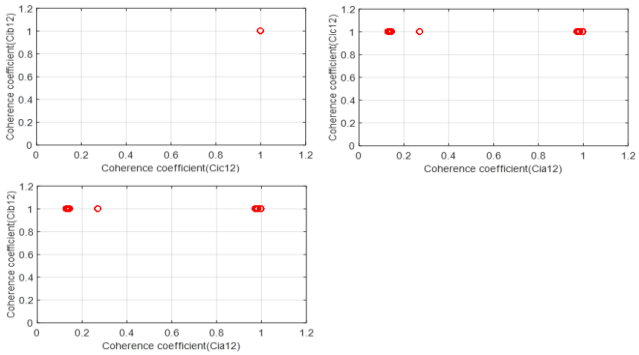

Fig. 11(d): Proposed scheme operating points on the tripping characteristics.

Fig. 11(a-d): Simulation results for case 4.

6. Advantages of the proposed differential current protection

The proposed scheme, for SG stator windings protection, has several advantages as given below:

(1) It is a novel protection scheme, based on the coherence analysis for the current signals measured at both SG stator windings terminals, against series and shunt faults,

(2) Only the 3-phase current measurements, at both SG stator windings ends, are required to implement this scheme,

(3) It can be processed on-line for faults detection and classification,

(4) It has closed tripping characteristics with a quadratic form, utilizing coherence coefficients, to determine the relay blocking and tripping zones for generator protection,

(5) It is simple, reliable and practical for protection of SG stator windings and the other power system elements,

(6) It has a fast response, (10 ms for a 50-Hz power system),

(7) The operation speed of the algorithm is controllable by the moving window used for calculating the coherence coefficients,

(8) It can adjust the pickup value of the coherence coefficients by selecting the coherent setting deviation,

(9) The algorithm's sensitivity is controllable via the coherence setting deviation and the moving data window size,

(10) It is not affected by the fault type, fault location, fault resistance, fault inception angle nor pre-fault power levels,

(11) Harmonics and DC components are digitally filtered with the data window used for computing the coherence coefficients,

(12) The coherence setting deviation and the data window concept can be used for amending the relay attributes such as security, dependability, stability, sensitivity and speed,

(13) The approach is able to differentiate between double line and double line-to-ground faults,

(14) Suitable for smart grid applications with different voltage levels for protecting the various power system components.

7. Conclusions

This paper presents a novel protection scheme based on coherence concept for SG stator windings. Six currents are measured at both SG stator windings ends which is sufficient to process this scheme. The coherence algorithm is used to detect, classify the fault, determine the faulty phase(s) and discriminate the location of fault, whether it is internal or external. New tripping characteristics, for the proposed protection algorithm, have been developed to determine the tripping and blocking zones for generator CB(s). In the proposed scheme, fault detection and identification have been performed in less than a half-cycle of the fundamental power frequency. The power system model, with real parameters, is simulated and verified using ATP and MATLAB software. The simulation results confirmed that the approach is smart, simple, reliable, accurate, fast and efficient at different operating and loading conditions. Also, the proposed algorithm is not affected by the fault type and location, fault resistance, fault inception time or pre-fault conditions. In addition, it can be practically implemented, with the availability to control the operation speed by adjusting the setting values of coherence coefficients according to the prevailed conditions of the power network. This makes the coherence approach a good candidate to compete with, or even to replace, the conventional numerical protection methods.

8. References

[1] El-Saadawi, M. Hatata: ''A novel protection scheme for synchronous generator stator windings based on SVM'', Journal of Protection and Control of Modern Power Systems, Vol. 2, Issue 24, PP. 1-12, Dec. 2017.

[2] Khaled Al Jaafari, Amir Negahdari and Hamid A. Toliyat: ''Modeling and experimental verification of a 100% stator ground fault protection based on adaptive third-harmonic differential voltage scheme for synchronous generators'', IEEE Transactions on Industry Applications, Vol. 53, Issue 4, PP. 3379-3386, March 2017.

[3] R. Gopinath, C. Santhosh Kumar, V. Upendranath, P.V.R. Sai Kiran, and K.I. Ramachandran: ''Intelligent fault diagnosis of synchronous generators'', Journal of Expert Systems with Applications, Vol. 45, Issue C, PP. 142-149, March 2016.

[4] N.W.Kinhekar, Sangeeta Daingade and Ajayshree Kinhekar: "Current differential protection of alternator stator winding", Paper submitted to the International Conference on Power Systems Transients (IPST2009) in Kyoto, Japan, June 3-6, 2009.

[5] Nader Safari-Shad, and Russ Franklin: ''Adaptive 100% stator ground fault protection based on sub-harmonic injection method'', Electrical Machines (ICEM), 2016 XXII International Conference on, 4-7 Sept. 2016.

[6] Dehkordi, A. B., D. S. Ouellette, and P. A. Forsyth: " Protection testing of a 100% stator ground fault using a direct-phase synchronous machine model in real time", In Developments in Power System Protection (DPSP 2010). Managing the Change, 10th IET International Conference on, PP. 1-5, 2010.

[7] Carlos Platero, and Miguel Pardo: ''Novel adaptive 100% stator ground fault protection based on the third harmonic measurement'', IEEE Conference Proceedings, Issue ICEM, PP. 2300-2305, Sep. 2016.

[8] R. Abd Allah: '' Unbalance current detection for synchronous generator using alienation concept '', International Journal of Engineering and Advanced Technology (IJEAT), Vol. 5, Issue 3, Feb. 2016.

[9] R. Abd Allah, S. M. Mohamed, E. H. Shehab-Eldin, and M. E. MASOUD: ''A new scheme based on correlation technique for generator stator fault detection-part II'', International Journal of Energy and Power Engineering. Vol. 3, Issue 3, PP. 147-153, 2014.

[10] R. Abd Allah, S. M. Mohamed, E. H. Shehab-Eldin, and M. E. Masoud: ''A new scheme based on correlation technique for generator stator fault detection-part I'', International Journal of Energy and Power Engineering. Vol. 3, Issue 3, PP. 116-124, 2014.

[11] A. Malhotra and P. Sharma: "Fault Detection and Classification Using Discrete Wavelet Transform", International Journal of Research and Innovation in

Social Science (IJRISS), vol. 7, no. 8, pp. 231–236, Aug. 2023.
[12] P. Malla, W. Coburn, K. Keegan, and X. H. Yu: "Power System Fault Detection and Classification Using Wavelet Transform and Artificial Neural Networks", in Advances in Neural Networks–ISNN 2019, vol. 11555, Springer, Cham, pp. 303–311, 2019.
[13] M. Hosseinzadeh, M. Rashidinejad, and H. Saadatmand: "A New Protection Algorithm for Synchronous Generators Using Artificial Neural Networks", IEEE Transactions on Power Delivery, vol. 38, no. 1, pp. 120-129, 2023.
[14] A. Ghosh, P. Sen, and S. Sharma: "Fuzzy Logic and Neural Network-Based Hybrid Protection Scheme for Synchronous Generator Stator Winding Faults", IEEE Transactions on Energy Conversion, vol. 39, no. 1, pp. 125-132, Mar. 2024.
[15] M. A. Saeed and M. El-Saadawi, "Practical Implementation of RNN-Based Synchronous Generator Internal Fault Protection", Recent Patents on Electrical & Electronic Engineering, vol. 12, pp. 181-189, 2019.
[16] K. Meena and K. K. Sahu: "Fuzzy Logic Controlled Neural Network for Fault Detection in Power Systems", IEEE Transactions on Power Delivery, vol. 38, no. 2, pp. 1345–1352, Apr. 2023.
[17] I. Jlassi and A. J. M. Cardoso: "Fuzzy Neural Network-Based Fault Diagnosis Method for Permanent Magnet Synchronous Generators", IEEE Journal of Emerging and Selected Topics in Power Electronics, vol. 8, pp. 2583-2599, 2019.
[18] A. F. Al-Hadhrami, S. M. Gupta, and M. S. Kumar: "A Novel Fault Detection Approach Using Fuzzy Logic and Neural Networks for Electrical Machines", IEEE Access, vol. 8, pp. 103656-103665, 2020.
[19] R. H. L. Lu, Y. C. Liao, J. M. Lin, and T. L. Lin: "Turn-to-Turn Fault Detection of Induction Motors Using Hybrid ANN and Fuzzy Logic System", IEEE Transactions on Industrial Electronics, vol. 67, no. 5, pp. 3946-3954, May 2020.
[20] H. Zhang, W. Yang, and Y. Zhang: "Support Vector Machine-Based Fault Classification for Electrical Machines Using Vibration Signals", IEEE Transactions on Industrial Electronics, vol. 71, no. 4, pp. 4003-4012, April 2024.
[21] J. A. Vargas, S. M. K. Wang, and L. R. Smith: "Fault Detection in Synchronous Generators Based on Independent Component Analysis and Machine Learning", IEEE Transactions on Energy Conversion, vol. 39, no. 2, pp. 789-798, June 2024.
[22] M. D. Martinez, F. G. Adams, and P. T. Williams: "Internal Fault Modeling of Synchronous Generators Using Voltage-Behind-Reactive Representation", IEEE Transactions on Power Delivery, vol. 39, no. 3, pp. 1625-1633, June 2024.
[23] Vilchis-Rodriguez, Damian S., and Enrique Acha: " A synchronous generator internal fault model based on the voltage-behind-reactance representation", Energy Conversion, IEEE Transactions on, Vol. 24, Issue 1, PP. 184-194, 2009.
[24] R. Abd Allah: ''Multifunction digital relay for large synchronous generators protection'', Ph.D. thesis, Helwan university, Chapter 3, 2012.
[25] R. A. Mahmoud: ''Integrated busbar protection scheme utilizing a numerical technique based on coherence method'', IET Journal of Engineering, vol. 2022, Issue 1, pp. 94–119, Jan. 2022.
[26] R. A. Mahmoud, A. Emam: ‘‘Coherence-based automatic power factor correction (APFC) algorithm for power grids’’, IET Journal of Engineering, vol. 2022, Issue 5, pp. 512–527, May 2022.
[27] R. A. Mahmoud, E. S. Elwakil: ‘‘Experimental investigations using quadratic-tripping characteristics based on alienation/coherence coefficients of voltage and current signals for synchronous generators protection’’, IET Generation, Transmission & Distribution, vol. 15, Issue 21, pp. 2978–3000, Nov.2021.
[28] R. A. Mahmoud: ''Coherence-based integrated detection and assessment algorithm for voltages and currents unbalance/disturbance in three-phase synchronous generators: A validation of simulation results'', IET Journal of Engineering, vol. 2023, Issue 5, pp. e12272, May 2023.
[29] R. A. Mahmoud: ''Smart automatic synchronization system based on coherence algorithm for power grids'', IET Journal of Engineering, vol. 2023, Issue 1, pp. e12214, Jan. 2023.

Appendix 1: Nomenclatures

Symbols	Abbreviations	Symbols	Abbreviations
$\Delta i_{s1}(n)$	change of secondary current $i_{s1}(n)$ at sample n for phase ''s'',	$i_{s2}(n)$	current signal (i_{s2}) at sample 'n' for phase 's' of the load SG stator winding terminal,
$\Delta i_{s2}(n)$	change of secondary current $i_{s2}(n)$ at sample n for phase ''s'',	I_{smax}	maximum value of secondary current of the current transformer,
3LG	Three line-to-ground fault,	N	samples per window,
ANN	Artificial Neural Network	N_f	sample at which the fault occurs,
ATP	Alternative Transient Program,	N_s	samples per cycle,
BB	Busbar	N_{sim}	total number of samples,
CB	Circuit breaker	N_T	current transformer turns ratio,
Ci	coherence coefficient for current signal,	R_b	current transformer burden
Ci_{a12}	coherence coefficient calculated between i_{a1} (n) and i_{a2} (n), same notation is used for phases "B and C"	R_{CT}	current transformer secondary winding resistance
Ci_{ab}	coherence coefficient calculated between i_{a1} (n) and i_{b1} (n),	R_f	fault resistance,
Ci_{bc}	coherence coefficient between i_{b1} (n) and i_{c1} (n),	R_{lead}	lead resistance
Ci_{ca}	coherence coefficient between i_{a1} (n) and i_{c1} (n),	R_n	Generator grounding impedance through the neutral point
Ci_{s12}	coherence coefficient between i_{s1} (n) and i_{s2} (n) for phase 's',	*S*	phase designation A, B, or C,
Ci_{sx}	coherence coefficient between i_{s1} (n) and i_{x1} (n) for phases 's and x',	*SLG*	Single line-to-ground fault,
CT	Current Transformer	t_f	fault inception time,
Cx	setting of coherence coefficient,	*TL*	Transmission line
DL	Double line fault,	*TW*	Travelling Wave
DLG	Double line-to-ground fault,	V_{1Max}	maximum phase voltage of SG,
F_{1op}	operating frequency of SG,	V_{2Max}	maximum phase voltage of the network,
F_{2op}	operating frequency of the electrical network,	$v_f(n)$	voltage of the fault point at sample n,
FD	Fault detection	V_n	nominal voltage of the power system
FL	Fault location	*VT*	Voltage Transformer
f_s	sampling frequency,	Z_f	The fault impedance,
h	sampling period,	α	power system angle,
$i_{a1}(n)$, $i_{a2}(n)$	instantaneous value of current signals at both SG stator windings terminals for phase 'A', the same notation is used for phases "B and C"	Δ	selected deviation of coherence setting,
$i_f(n)$	total short circuit current, at sample n,	δ_1	operating power angle of synchronous generator,
I_{max}	maximum value of the primary current of the CT,	δ_2	operating power angle of the electrical network,
I_n	nominal current of the power system	ω	angular velocity of the power system,
$i_{s1}(n)$	current signal (i_{s1}) at sample 'n' for phase 's' of the neutral SG stator winding terminal,	θ	fault inception angle,

Appendix 2: Pre-fault operating conditions of the simulated power system for each case study.

Electrical Component (Operating Condition)	Data
Operating peak phase voltage of synchronous generator	16.063 kV
Operating peak phase voltage of Electrical power network	16.063 kV
$F_{1operated}$ of synchronous generator	50 Hz
$F_{2operated}$ of electrical power network	50 Hz
Synchronous generator operating power angle (δ_1)	0^o
Electrical power network operating power angle (δ_2)	0^o
Generator grounding impedance	1.0 Ω
Electrical Load 1	1 + j 0.53 Ω
Electrical Load 2	10.85 + j 6.72 Ω
CB_{11}, CB_{12}, CB_{13}, CB_{21}, CB_{22} CB_{23}, CB_{24} and CB_{33} status	Close

Appendix 3: Parameters' data of the simulated power system.

Power system parameter	**Data**
Machine 1 (Sending source):	
Rated Volt-ampere	*320 MVA*
Rated line voltage	*19 kV*
voltage phasor angle	*0^0*
Rated frequency	*50 Hz*
Number of poles	*2*
Neutral grounding impedance (R_n)	*1.0 Ω*
Power Network (Receiving source):	
Nominal line voltage	*500kV (1pu)*
Voltage phasor angle phase	*0^0*
Nominal frequency	*50 Hz*
Volt-ampere short circuit	*25 GVA ($i_{s.c}$ = 10 kA)*
Main Transformers:	
Rated Volt-ampere	*340 MVA*
Transformation voltage ratio	*19.57 kV /500 kV*
Connection primary/secondary	*Delta/Star earthed neutral*
Primary winding impedance (Z_p)	*0.0027 + j0.184 Ω*
Secondary winding impedance (Z_s)	*0.7708 + j 61.8 Ω.*
Vector group	*YNd1*
Z%	*15%*
Transmission Lines (1&2):	
+ve sequence R	*0.0217 Ω /km*
Zero sequence R	*0.247 Ω /km*
+ve sequence XL	*0.302 Ω /km*
Zero sequence XL	*0.91 Ω /km*
+ve sequence 1/Xc	*3.96 µŬ /km*
Zero sequence 1/Xc	*2.94 µŬ /km*
Transmission line long (Km)	*200 Km*
Main Load (load 1):	
Load 1 Volt-ampere	*25 GVA at PF = 0.85 lag*
Aux. Load (load 2):	
Load 2 Volt-ampere	*30 MVA at PF = 0.85 lag*
Current Transformer (CT):	
Current Transformer Ratio	*12000/1*
Rated burden	*30 VA*
Class	*5p20*